

# CURVED FENCES FOR PART ALIGNMENT

Mike Brokowski, Michael Peshkin  
 Department of Mechanical Engineering  
 Northwestern University  
 Evanston, Illinois 60208-3111

Ken Goldberg  
 Department of Computer Science  
 University of Southern California  
 Los Angeles, California 90089-0273

## Abstract

In automated packing or assembly it is often necessary to bring randomly oriented parts into uniform alignment. Mechanical methods such as vibratory bowl feeders are often used for this purpose, although there is no theory for the systematic design of such feeders. A slanted "fence" attached to the stationary sides of a conveyor belt is also capable of orienting a stream of parts and a sequence of such fences has been shown [14] to function as a systematically designable linear parts feeder.

A limitation of fence alignment is that once a part has left contact with a fence, its final orientation is confined to a narrow range of angles but is not unique. Here we consider the design of an individual fence, consisting of a straight slanted section followed by an optimal curved tail. The straight section selectively aligns certain edges of the part, while the curved tail preserves this alignment precisely as the part leaves contact with the fence. We have found the shortest tail which guarantees alignment.

## 1. Introduction and Background

In robotics and in manufacturing operations involving packing or assembly, parts commonly move down an assembly line on a conveyor belt before being grasped. It is often necessary to orient the parts accurately so that they may be reliably grasped. Parts feeders perform this function by taking parts from random orientations to a unique one. Figure 1 shows an example conveyor belt using fences to orient parts.

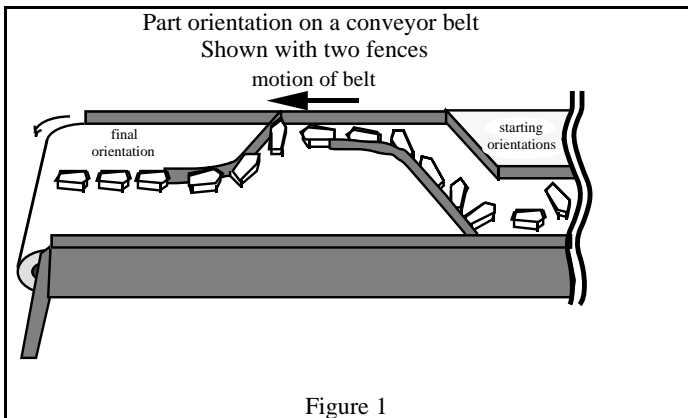


Figure 1

When the corner of a part hits a fence the part rotates until a flat edge is aligned with the fence, and then continues to slide down the fence on that edge. As the part leaves the fence, it turns further as it interacts with the curved tail of the fence. It stops turning as it loses contact with the fence, and does not rotate until it contacts the next fence.

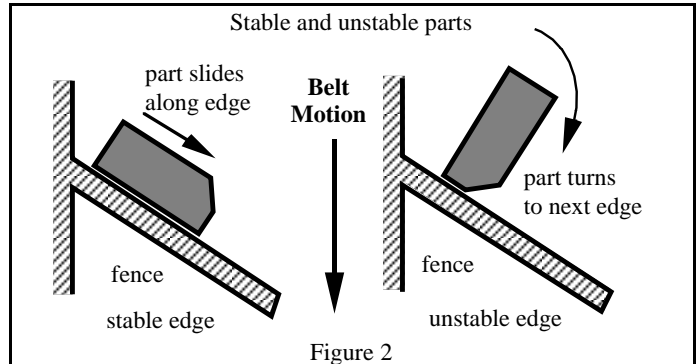


Figure 2

As Figure 2 illustrates, only certain edges of a part are *stable*, meaning that the part can slide along a fence on that edge without turning onto the next edge.

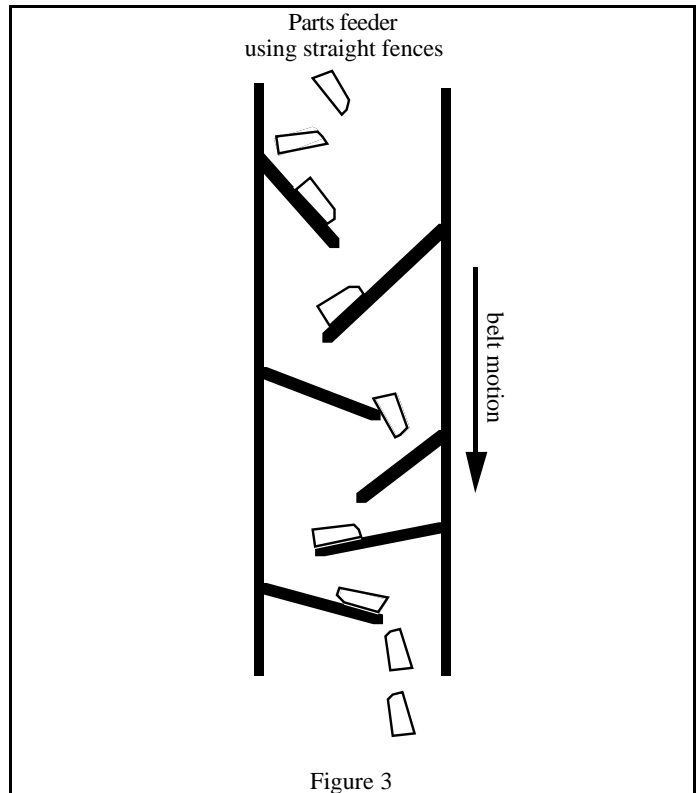


Figure 3

Although in general several different edges of a part are stable, by arranging a *sequence* of fences at appropriate angles, one can ensure that a single unique edge of all parts rests against the final fence, so that all parts leave the final fence from that same edge. Figure 3 shows a parts feeder based on this concept (from [14]).

Optimal curved fences for part alignment on a belt

Mike Brokowski, Michael A. Peshkin, Ken Goldberg

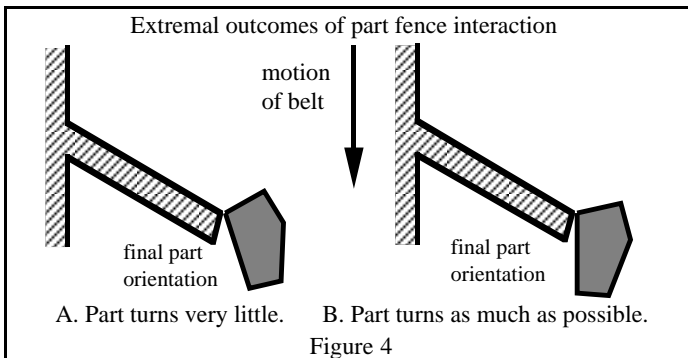
ASME Journal of Mechanical Design, 117 (1), March 1995 (p. 27)

Mason [10] was the first to analyze the role of *pushing* in robot manipulation. Building on results from classical mechanics, he identified a fundamental rule for predicting the sense of rotation (CW or CCW) of a part as it is pushed in the presence of Coulomb friction. Other geometric methods for predicting part motion in the presence of frictional contacts were described in [5], [6], [16], [3], and [2]. Mason's rule provided the basis for Brost's [1] *push diagram*, which represents all possible motions of a part as it is grasped by a parallel-jaw gripper.

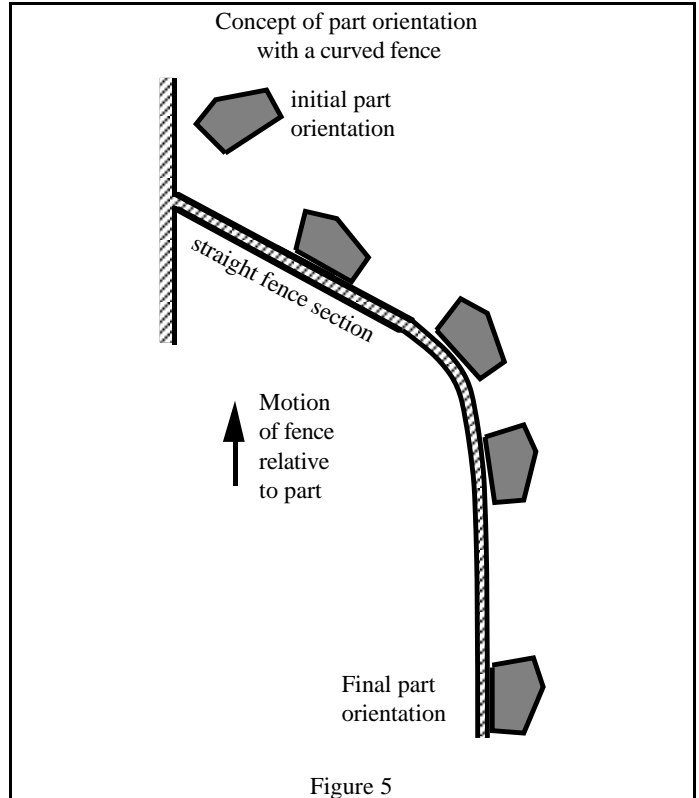
When there is greater uncertainty in the initial orientation of a part, more than one action may be required to construct a sensorless orienting strategy. Several researchers have addressed the problem of finding a *sequence* of actions (a multi-stage plan) for orienting polygonal parts. Mani and Wilson [9] considered pushing actions using a single planar fence. Peshkin and Sanderson [14] considered pushing with an arrangement of fixed fences on a conveyor belt. Erdmann and Mason [6] considered tilting actions that cause a part to slide into contact with the edges of a rectangular tray. Goldberg and Mason [8] considered grasping actions using a parallel-jaw gripper. In each case the authors partitioned the set of possible actions into a finite number of equivalence classes based on part geometry. (Christiansen [4] describes how automated experiments, in lieu of mechanical analysis, can be used for this purpose.) Each applied a breadth-first exhaustive search to find a sequence of actions guaranteed to produce a unique final orientation of the part. Each method is complete in the sense that it is guaranteed to find such a plan if one exists.

Goldberg [7] described an  $O(n^2)$  algorithm for finding a sequence of grasp actions that will orient a given polygonal part, and he proved that such a sequence exists for any polygonal part. There is some evidence that this algorithm can be modified for the automatic design of Peshkin-type fence arrangements for conveyor belt feeders. However, the algorithm assumes that each fence will produce a finite set of part orientations rather than the continuous range obtainable by straight fences.

Here we focus on one aspect of the belt-based feeder shown in Figures 1 and 3. Our problem with the belt-based system is that, due to small variations in contact geometry, all parts leaving a straight fence emerge in a range of orientations (typically  $\pm 10^\circ$ ) instead of in a unique orientation. Figure 4 shows the cause: some parts turn little as they leave a fence (4A) and some turn more (4B). When the part edge sliding on the fence leaves parallel to the belt's direction of motion we refer to that part as *aligned* with the belt's motion. A convex part cannot turn beyond alignment with the belt motion.



In this paper we solve the problem of parts leaving fences unaligned with belt motion by attaching a curved section of fence (a "tail") to the end of the straight fence. An optimal tail reorients the edge of the part that was sliding along the fence as quickly as possible, until it is aligned with the direction of motion of the belt. Figure 5 shows such a curved section.

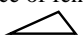
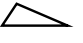


## 2. Contribution of this work

We will find the optimal (most compact) fence shape that nevertheless guarantees a part will leave the end of a fence aligned with the belt motion, with arbitrarily small orientational error.

Note that this problem is equivalent to one where a part sits upon a stationary surface while a fence moves by and pushes it into alignment. The fence motion *relative* to the part is the important characteristic. In analyzing the problem, it is simpler to look at the case where the fence moves.

Our analysis assumes several things.

- The outline of the part will be described as a convex polygon. Concave edges can be accommodated but will not be discussed here.
- We consider only parts moving on a flat surface and being pushed near their bottoms.
- All motion occurs in the plane, so no sequence of fences can flip a part over, e.g. from this configuration  to this one .

- We assume frictionless contact between the part and the fence. However, this is a *conservative* assumption; these fences still work in the presence of friction.
- We assume that the motion of the parts is *quasi-static* [11] [15]; that is, mass  $\times$  acceleration is small compared to the frictional forces acting upon a part.
- There are no collisions between parts; we do not address the problem of isolating parts (*singularizing*).

In previous work we have shown that we can take a part from any random initial orientation to a unique final orientation *range* using a sequence of straight fences. Here, we focus on reducing that range of final orientations by developing curved fences whose ranges are arbitrarily small. Our solutions determine the most compact curved shape which guarantees alignment based upon three part parameters describing part geometry (section 3) and a more conservative, universal shape which scales simply to guarantee alignment (section 4) for any part.

### 3. Optimal Curved Fences

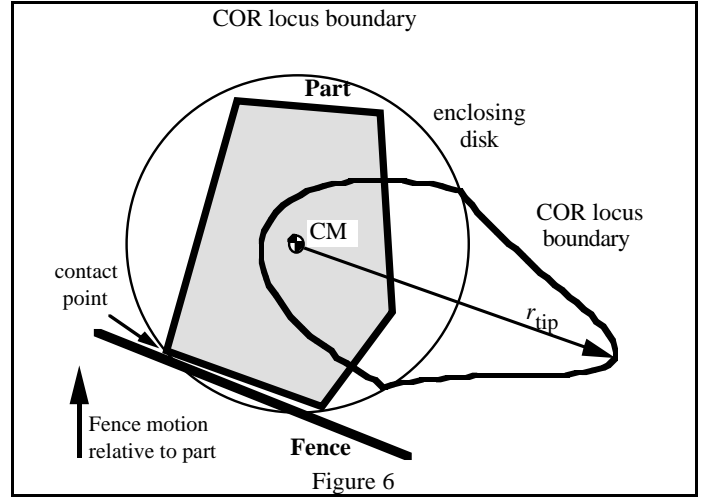
#### 3.1 Uncertainty in Part Motion

To determine how to design fences which orient parts, we first look at how a part moves when pushed by a fence. This subsection incorporates Mason's results [12] for the motion of a pushed part and Peshkin's results [13] bounding part motion in the presence of uncertainty to examine the motion of a part pushed by a fence.

Peshkin has shown that how a part moves depends on the *pressure distribution* between the part and the surface upon which it moves. This distribution can vary with surface flatness or "bumps" and introduces uncertainty into the part's motion. Noting that a part sliding on a planar surface has three degrees of freedom and it has only two degrees of freedom when required to remain in contact with its pusher, we can characterize the part's motion by the location of its instantaneous *center of rotation (COR)* so that any infinitesimal motion of the part is a pure rotation  $\delta\theta$  about its COR.

Since we wish to determine the motion of any part without knowing its exact pressure distribution, which may vary from part to part in any case, we can determine all of the *possible* CORs for a given part [13] over all possible pressure distributions. We can bound the CORs for a given part, regardless of pressure distribution, within an area of the plane called the *COR locus*.

By choosing a disk centered at the part's center of mass (CM) and large enough to enclose the entire part, we guarantee that any pressure distribution that the part might have is also one that the disk might have. Therefore, by determining the COR locus of the disk, we bound the COR locus of the part. Previous work reveals the shape of this locus, whose exact form [13] needn't concern us here, and Figure 6 shows the boundary of the COR locus for a typical part pushed by a section of fence.

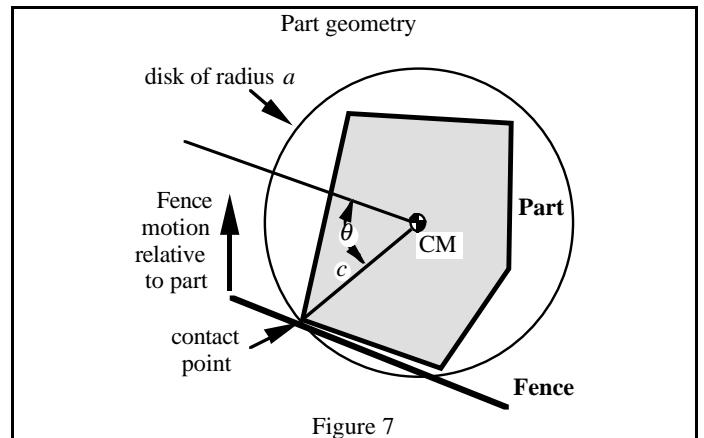


Shown in this figure and of particular interest is  $r_{tip}$ , the distance from the CM to the most distant point in the COR locus. This point represents the slowest possible turning for a part of this shape. The vector  $r_{tip}$  is parallel to the fence at the contact point.

Peshkin has shown [13] [14] that

$$r_{tip} = \frac{a^2}{c \cos \theta} \quad (1)$$

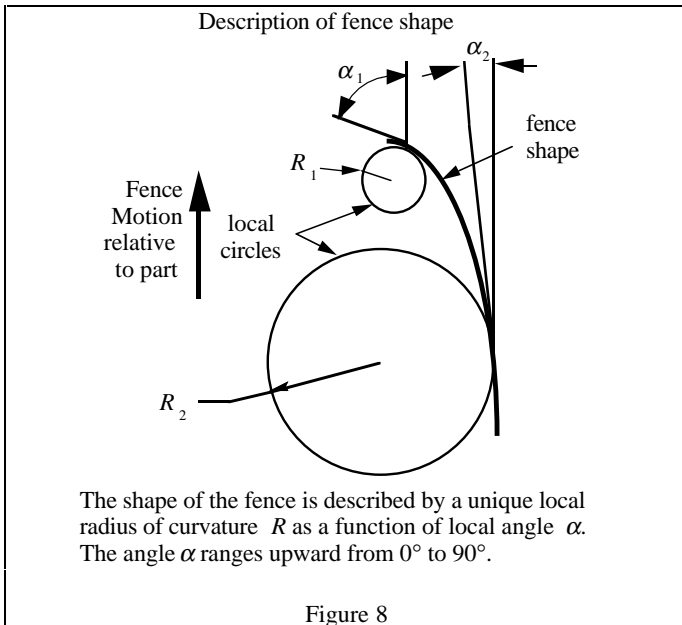
where  $c$  is the distance from the CM to the contact point,  $a$  is the radius of the enclosing disk mentioned before, and  $\theta$  is the angle from the line  $c$  to a line parallel to the fence at the contact point. These parameters are shown in Figure 7 below. Notice that  $c/a$  cannot exceed unity. Also, for any rectangle of uniform density,  $c/a = 1$ .



Parts that turn about CORs in the rest of the COR locus will rotate more and slide less than the slowest turning parts, which rotate about  $r_{tip}$ . A fence will not have any trouble pushing them into alignment if it can push the slowest turning parts into alignment.

We assume here that there is no friction between the part and the pusher. We can treat the frictional case but we will explain later that  $\mu_c = 0$  is the conservative assumption.

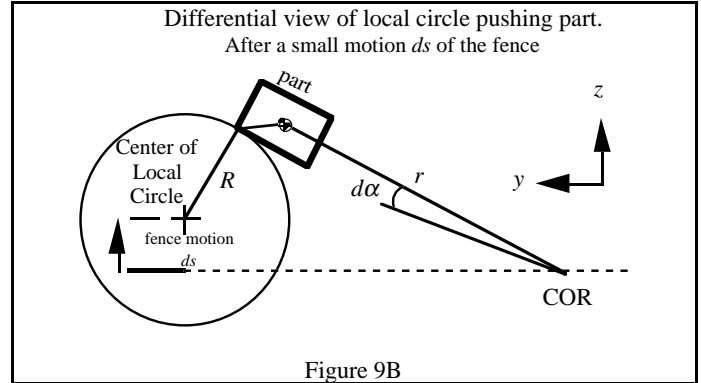
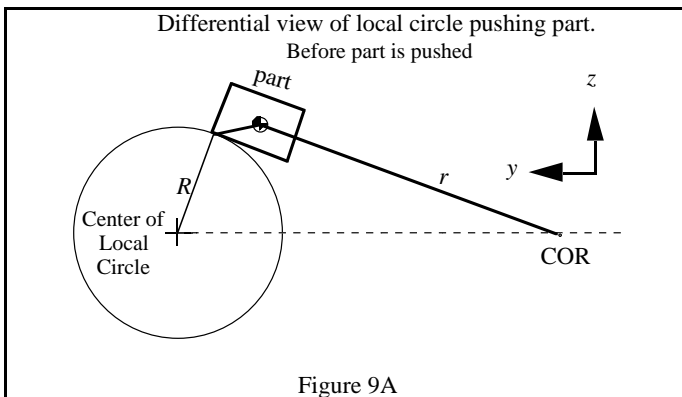
### 3.2 Determining Exact Fence Shapes



Now that we know how our worst case (slowest turning) part can move, we can construct a fence shape that will turn it. We describe our curved fence in  $(\alpha, R)$  coordinates.  $\alpha$  is the angle (local slope) of the fence and  $R$  is the local radius of curvature of the fence.  $\alpha$  is measured with respect to the fence's direction of motion as shown in Figure 8. Notice that, at a given angle  $\alpha$ , a smaller  $R$  describes a sharper curve in the fence and a larger  $R$  describes a less sharp curve.

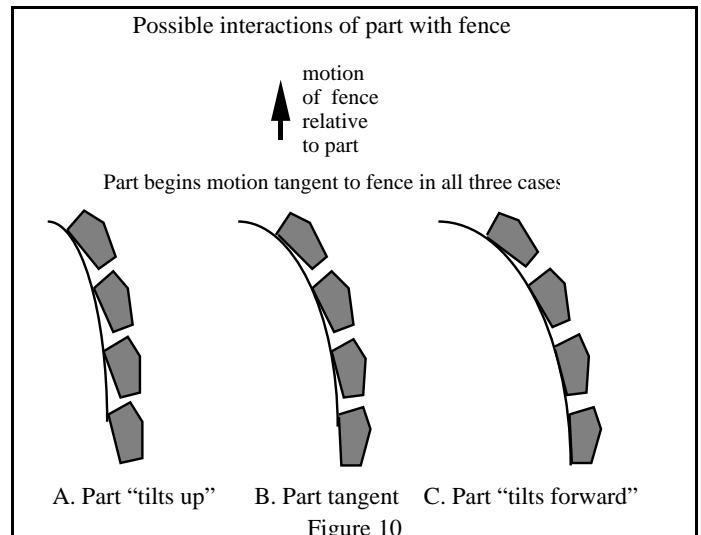
By using this description of the fence shape, we can replace a segment of fence by a "local circle": a circular pusher of the same local radius of curvature. We can then address the simpler question of how the radius  $R$  of the circular pusher depends on the angle  $\alpha$  at which the part is pushed. The answer to this central question determines the shape of our curved fence.

Figures 9A-B shows a differential view of this problem. The fence, represented by its local circle, moves straight up, pushing the part ( $ds$ ), which rotates  $d\alpha$  about its center of rotation (COR) (Figure 9B). Here  $r$  is the length of the line from the part's CM to the COR.



Now we can describe the part's motion as it is pushed by a fence. When our most slowly turning part is pushed by a fence of a local radius of curvature  $R$  at an angle  $\alpha$ , it will rotate about a particular COR. This geometry problem gives us the relationship between four variables:  $R$ ,  $\alpha$ , and the location ( $y$  and  $z$  coordinates) of the COR. By imposing two mathematical conditions forcing our fence to accommodate the worst case part, we can eliminate two of these variables – the location of the COR. This allows us to determine the relationship between  $R$  and  $\alpha$ , which describes the optimal fence shape.

First, we require that for the most slowly turning part, the trailing end of the part's aligned edge will begin and remain tangent to the contact point on the fence. Figure 10B shows this *condition on tangency*, as do Figures 9A-B above. If the part turned more quickly than this, then it would simply be aligning itself more quickly by "tilting forward" on the fence (Figure 10C). If the part turned more slowly it might not keep up with the fence and begin "tilting up" on the fence without any way of assuring that the fence could push it back into alignment (Figure 10A). Accommodating the most slowly turning part assures that all parts will leave the fence, at worst, aligned with the slope of the end of the fence and, at best, aligned with the fence's direction of motion. By extending the curved section of fence, we can make the difference between these two extremes arbitrarily small.



The condition on tangency allows us to solve part of the geometry problem mentioned above and illustrated in Figures 9A-B. Suppose the part is initially tangent to the circle and remains tangent as it rotates about its COR. We might as well imagine that the circle is rigidly attached to the part, moving with the part as the part turns. The center of the circle moves straight up. This implies that the COR lies on a line perpendicular to the circle's upward motion and passing through the center of the circle. So, by using the condition on tangency, we have one constraint on the COR's location — the COR must lie along the dashed horizontal line shown in Figure 9B.

Our second condition is *slowest part accommodation*. We want to accommodate the most slowly turning part because any faster turning part will align itself anyway. This means that the conservative COR is the one for the slowest turning part;

$$r = r_{\text{tip}} \quad (2)$$

Our slowest part accommodation condition tells us where exactly on the dotted line the COR lies. Since equation (1) gives an expression for  $r_{\text{tip}}$  in terms of part geometry, we can solve for the relationship between  $R$  and  $\alpha$ . We find this to be

$$R = \frac{1}{\tan(\alpha)} \left( \frac{a^2}{c \cos(\theta)} + c \cos(\theta) \right) - c \sin(\theta) \quad (3)$$

This equation describes the shape of the fence in the  $(R, \alpha)$  coordinates depicted in Figure 8. To convert these to more familiar orthogonal  $(y, z)$  coordinates, we can substitute for  $\alpha$  and  $R$ . These substitutions reveal a second order ordinary differential equation:

$$\frac{d^2y}{dz^2} = \frac{(1 + (dy/dz)^2)^{3/2}}{\frac{a^2}{c (dy/dz) \cos(\theta)} + \frac{c \cos(\theta)}{(dy/dz)} - c \sin(\theta)} \quad (4)$$

Equation (4) gives the exact shape of the optimal fence curve in orthogonal coordinates and we solve it numerically. By solving the equation from  $\alpha \approx 90^\circ$  ( $dy/dz \approx \infty$ ) until  $\alpha$  has reached some sufficiently small value ( $\alpha_{\text{final}}$ ), we bound the variation of the final part's orientation so that its aligned edge will lie between  $\alpha_{\text{final}}$  and  $0^\circ$  from the fence's direction of motion.

A detail we encounter with exact fence shapes is that we cannot start the curved section of a fence quite at  $\alpha = 90^\circ$  due to a cusp in equation (4). It can be shown that the highest angle  $\alpha$  where a fence solution may start is where the contact point is level with the COR:

$$\tan(\alpha_{\text{max. start}}) = \frac{(a/c)^2}{\cos(\theta) \sin(\theta)} + \frac{\cos(\theta)}{\sin(\theta)} \quad (5)$$

In most instances, friction will render high starting values of  $\alpha$  impossible anyway because the part would stick on the straight section of fence. We can minimize  $\alpha$  in equation (5) with respect to  $(c/a)$  and  $\theta$ . As a result, the lowest (worst) value for  $\alpha_{\text{max. start}}$  is  $\sim 70.53^\circ$  and occurs at  $\theta \approx 55^\circ$  and  $c/a = 1$ . Any exact fence starting at this angle, regardless of part geometry, will have no cusp.

We have assumed frictionless contact between the fence and the part. Any  $\mu_c > 0$  will cause the part to turn more quickly than it would with zero friction, causing it to align itself with the fence more quickly, which is fine. Of course, if  $\mu_c$  is too high, the aligning side

will be unstable and the part will tumble over the leading edge and onto its next side. It can be shown that if the straight section of fence is stable, so too will be any curved section attached to it.

Figure 11 shows an exact fence curve generated for a square part using equations (4). This fence starts at  $\alpha = 71.57^\circ$  and ends at  $\alpha = 1^\circ$ . The square shown is drawn to scale and shows that, to align this part to within  $1^\circ$ , the fence's  $y$  dimension must extend to about 1.1 times the square's width. Exact fence shapes scale directly with part size  $a$  as we expect so that, to accommodate a square twice the size of the one shown, we would merely double the dimensions of the fence.

Figure 11 also shows a dashed line representing a straight section of fence. A curved section of fence may be attached tangent to a straight section at any angle.

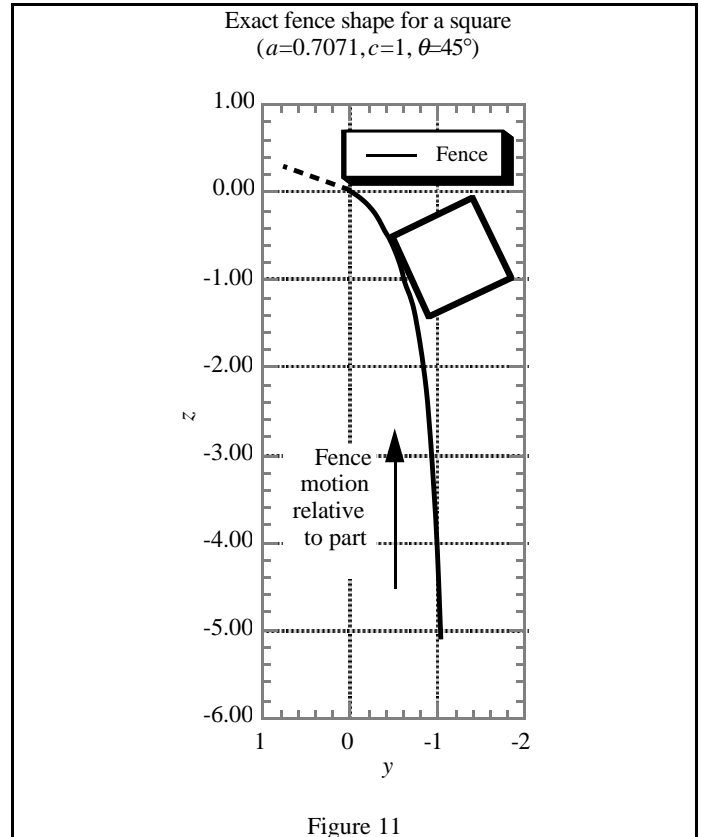


Figure 11

#### 4. A “Universal” Fence Shape

The fences described by equations (3) and (4) depend on three parameters which account for particular part geometry. Further, these equations result in a different *shape* for different part parameter values  $\theta$  and  $c$ . That is, we cannot simply take the shape generated for a part with a particular  $\theta$  and scale it to fit a part with a different  $\theta$ . We would like to determine a single fence shape that is guaranteed to work for all parts, or a *universal* fence, by making conservative assumptions about part interaction with the fence.

Examining equation (3), we see that the last term,  $-c \sin(\theta)$ , will always be negative and therefore will always reduce  $R$  at a given  $\alpha$ . Since a larger  $R$  describes a less sharp curve, which is easier for a part to follow, we can safely neglect this term and have less sharp fences that will still align parts, albeit more slowly and

conservatively than necessary. Thus, the equation describing a universal shape is

$$R = \frac{k}{\tan \alpha} \quad (6)$$

where

$$k = \frac{a^2}{c \cos(\theta)} + c \cos(\theta). \quad (7)$$

is a *characteristic part number*: a factor by which the single universal shape described by (6) can be simply scaled to align a particular part. The parameters  $\theta$ ,  $c$ , and  $a$  are shown in Figure 7. The minimum  $k$  for any part is  $2a$ , and occurs when  $c = 1$  and  $\theta = 0^\circ$ .

Equation (6) describes a *universal* shape which will align any part. By this we mean that the one *shape* described by equation (6) will work for all parts;  $k$  is simply a scaling factor. Moreover, since a larger  $R$  is conservative, a part with characteristic part number  $k_1$  will also be aligned by a fence scaled by  $k_2$  if  $k_2 > k_1$ .

We can substitute for  $R$  and  $\alpha$  in equation (6) to find the differential equation describing this fence in orthogonal coordinates:

$$\frac{d^2y}{dz^2} = \frac{(dy/dz)(1 + (dy/dz)^2)^{3/2}}{k} \quad (8)$$

Equation (8) may be solved to find  $z$  as a noninvertible function of  $y$ . If our fences start at the origin, we find this function to be

$$\frac{z}{k} = \sqrt{-(y/k)^2 - 2(y/k)} + \frac{1}{2} \ln \left( \frac{1 - \sqrt{-(y/k)^2 - 2(y/k)}}{1 + \sqrt{-(y/k)^2 - 2(y/k)}} \right) \quad (9)$$

We note that both  $y$  and  $z$  always appear normalized by  $k$ . Any fence generated for  $k = 1$  can be made to work for any other  $k$  simply by scaling the shape along the  $y$  and  $z$  axes.

Unlike the exact optimal fence shape described in the previous section, these universal fences are well behaved at  $\alpha = 90^\circ$  and it is not necessary that a fence generated this way start at an angle less than  $90^\circ$ . Even the most slowly turning parts on this conservative fence are turning more quickly than the fence and, instead of remaining tangent to it, they “tip forward” as shown in Figure 10C.

Now, the universal fence shape shown in Figure 12 is scaled for a square part of side length 1, for which  $k = 3/2$ . Here  $\alpha$  starts at  $90^\circ$  and ends at  $1^\circ$ . Shown near the top left of the fence at  $\alpha = 57^\circ$  is a section of straight fence attached tangent to the fence. A curved section of fence can be attached tangent to any straight section of fence to guarantee alignment of stable parts leaving that fence.

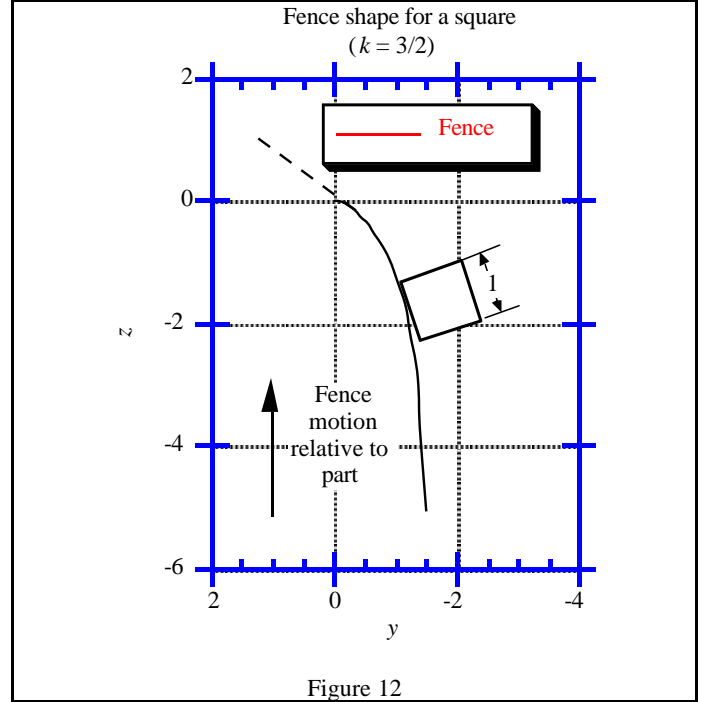


Figure 12

Of concern to us in practical uses of the fence is how wide ( $y$ ) a fence must be to guarantee a part's orientation to a required angular tolerance. For example, Figure 12 shows that, to get the square within  $1^\circ$  of alignment, the fence width must be roughly 1.5 times the length of the square's sides, which is slightly wider than the exact fence generated for the same square in Figure 11. As our tolerance  $\alpha_{\text{final}} \rightarrow 0^\circ$ , equation (9) asymptotically approaches a finite value  $-k$ . In practice, we do not want infinitely long fences. The relationship between the fence angle  $\alpha$  and the width of the fence at that point is given by

$$\tan \alpha = \frac{dy}{dz} = \frac{y + k}{\sqrt{-2ky - y^2}} \quad (10)$$

$$\text{or} \quad y = k (\sin \alpha - 1) \quad (11)$$

We can use equation (11) to determine how wide a fence must be to guarantee part alignment. Of course, we can also determine how long ( $z$ ) a fence will be using equation (9).

## Conclusions

We have found the optimal class of fence shapes for use in belt-based parts feeders that orient parts to within an arbitrarily small range. Fences of this design guarantee that a part will move into proper orientation regardless of the specific pressure distribution between the part and the surface upon which it slides. They are optimal in that they are the most compact shapes guaranteed to align parts. The optimal shape for a given curved section of fence can be generated automatically based upon three simple geometric parameters of the part via equation (4). This curved section of fence may be attached to a straight section of fence for use in parts feeder design.

We have also defined a characteristic part number  $k$  and developed a more conservative but slightly less compact single fence shape

which scales simply with  $k$ . This universal fence shape, described by equation (9), can be scaled with  $k$  to guarantee alignment for all parts. As with the exact fence shapes, the curved section of this type of fence may be attached to any straight section of fence.

## Acknowledgments

We wish to thank Northwestern University and the National Science Foundation (NSF grant DMC 8857854) for supporting this work, and William L. Kath for assistance in solving equation (8).

## References

1. Brost, R. C. *Automatic Grasp Planning in the Presence of Uncertainty*. International Journal of Robotics Research (February)(1988)
2. Brost, R. C. *Analysis and Planning of Planar Manipulation Tasks*. PhD, Carnegie Mellon University (1991)
3. Brost, R. C. ; M., Matthew T. *Graphical Analysis of Planar rigid body dynamics with multiple frictional contacts*. 5th International Symposium on Robotics Research. (1989)
4. Christiansen, A. D. *Automatic Acquisition of Task Theories for Robotic Manipulation*. PhD, CMU School of Computer Science (1991)
5. Erdmann, M. A. *On motion planning with uncertainty*. MS Thesis, Massachusetts Institute of Technology (1984)
6. Erdmann, M. A. and M. T. Mason. *An Exploration of Sensorless Manipulation*. IEEE International Conference on Robotics and Automation. (1986)
7. Goldberg, K. Y. *Orienting polygonal parts without sensors*. Algorithmica (1992)
8. Goldberg, K. Y. and M. T. Mason. *Bayesian Grasping*. IEEE International Conference on Robotics and Automation. (1990)
9. Mani, M., Wilson, W. R. D. *A Programmable Orienting System for Flat Parts*. North American Manufacturing Research Institute Conference XIII. University of California, Berkeley (1985)
10. Mason, M. T. *Manipulator Grasping and Pushing Operations*. PhD thesis, MIT (1982)
11. Mason, M. T. *On the Scope of Quasi-static Pushing*. 3rd International Symposium on Robotics Research. (1985)
12. Mason, M. T. *Mechanics and planning of manipulator pushing operations*. The International Journal of Robotics Research **5**(3):53-71 (1986)
13. Peshkin, M. A. and A. C. Sanderson. *The Motion of a Pushed, Sliding Workpiece*. IEEE J. Robotics and Automation **4**(6):569-598 (1988)
14. Peshkin, M. A. and A. C. Sanderson. *Planning Robotic Manipulation Strategies*. IEEE J. Robotics and Automation **4**(5)(1988)
15. Peshkin, M. A. and A. C. Sanderson. *Minimization of Energy in Quasistatic Manipulation*. IEEE J. Robotics and Automation **5**(1):53-60 (1989)
16. Rajan, V. T. ; B., R.; Schwartz, J. T. *Dynamics of a rigid body in frictional contact with rigid walls*. IEEE Conference on Robotics and Automation. (1987)